

AperTO - Archivio Istituzionale Open Access dell'Università di Torino

A Jurassic oceanic core complex in the high-pressure Monviso ophiolite (western Alps, NW Italy)

This is the author's manuscript

Original Citation:

Availability:

This version is available <http://hdl.handle.net/2318/1523566> since 2018-06-14T11:45:25Z

Published version:

DOI:10.1130/L458.1

Terms of use:

Open Access

Anyone can freely access the full text of works made available as "Open Access". Works made available under a Creative Commons license can be used according to the terms and conditions of said license. Use of all other works requires consent of the right holder (author or publisher) if not exempted from copyright protection by the applicable law.

(Article begins on next page)



UNIVERSITA' DEGLI STUDI DI TORINO

This is an author version of the contribution published on:

Questa è la versione dell'autore dell'opera:

Festa, A., Balestro, G., Dilek, Y., Tartarotti, P. (2015) -Lithosphere, v.7, 646-652

doi: 10.1130/L458.1.

The definitive version is available at:

La versione definitiva è disponibile alla URL:

<http://lithosphere.gsapubs.org/>

20
21
22
23
24 **A Jurassic Oceanic Core Complex in the High-P Monviso Ophiolite**
25 **(Western Alps, NW Italy)**
26

27
28 ¹Andrea Festa, ^{1*}Gianni Balestro, ²Yildirim Dilek, and ³Paola Tartarotti
29

30
31 1: Dipartimento di Scienze della Terra, Università di Torino, Via Valperga Caluso, 35, 10125 - Torino,
32 Italy

33 2: Department of Geology and Environmental Earth Science, Miami University, Oxford, OH 45056,
34 USA

35 3: Dipartimento di Scienze della Terra, Università di Milano, Via Mangiagalli, 34, 20133 - Milano,
36 Italy
37
38
39
40
41
42
43
44
45
46
47
48
49
50
51
52

53 ***Corresponding author:**

54 Gianni Balestro

55 E-mail: gianni.balestro@unito.it

56 Phone: +39-0116705865
57
58
59
60
61
62
63
64
65

66 LITHOSPHERE (Short Research Contributions)
67

Abstract

The eclogite-facies Monviso ophiolite (MO) in the Western Alps displays a complex record of Jurassic rift–drift, subduction zone and Cenozoic collision tectonics in its evolutionary history. Serpentinized lherzolites intruded by 163 ± 2 Ma gabbros are exposed in the footwall of a thick shear zone (Baracun Shear Zone = BSZ), and are overlain by basaltic lava flows and syn-extensional sedimentary rocks in the hanging wall. Mylonitic serpentinites with sheared ophicarbonates veins and talc-, and-chlorite-schist rocks within the BSZ represent a rock assemblage that formed from seawater-derived hydrothermal fluids percolating through it during intra-oceanic extensional exhumation. Lower Cretaceous calcschist, marble and quartz-schist metasedimentary assemblage unconformably overlies the footwall – hanging wall units, representing a post-extensional sequence. The MO, BSZ and the associated structures and mineral phases represent a core complex formation (OCC) in an embryonic ocean (i.e., the Ligurian-Piedmont Ocean). The heterogeneous lithostratigraphy and the structural architecture of the MO documented here are the products of rift-drift processes that were subsequently overprinted by subduction zone tectonics, and may also be recognized in other (ultra)high-P belts worldwide.

Key words: Western Alps; oceanic core complex; extensional tectonics and detachment faults; Jurassic Monviso ophiolite; syn-extensional and post-extensional sedimentary sequences.

Introduction

Submersible surveys, geophysical studies, and deep ocean drilling projects during the last two decades have provided new insights into the mode and nature of magmatic, tectonic and hydrothermal processes that occur along slow- to ultraslow-spreading ridges (e.g., Cannat, 1993; Tucholke et al., 1998; Dilek, 2000; Karson et al., 2006). These studies have revealed the occurrence on the seafloor of oceanic detachment faults and associated shear zones with deformed mafic-ultramafic rocks. Detachment faults along non-volcanic rifted margins and in young oceanic lithosphere accommodate high-magnitude extension causing the exhumation of lower crustal gabbros and upper mantle peridotites on the seafloor, forming oceanic core complexes (OCCs; Cannat et al., 2006; Karson et al., 2006; Smith et al., 2014). These rocks display mineral assemblages and structural fabrics, developed during the interplay of ductile and brittle deformation episodes, fluid-rock interactions, and metasomatism associated with their exhumation (Boschi et al., 2006).

Recognition of detachment faults and core complex structures in fragments of ancient oceanic lithosphere is often difficult because of multi-stage, intense deformation and metamorphism they experienced during subduction and subsequent continental collision-related exhumation. Yet, slivers of mafic-ultramafic rock assemblages in collision zones have been widely used in numerous studies to document the occurrence of remnants of oceanic basins and to reconstruct their paleogeographies in the geological past (Decandia and Elter, 1972; Lagabrielle, 1994; Dilek and Thy, 1998; Manatschal et al., 2011; Balestro et al., 2014; Dilek and Furnes, 2014). However, results of such reconstructions may lead to misleading interpretations for the tectonic settings of the investigated ophiolites and for the extent of the inferred ocean basins in which they formed, if the primary seafloor structures of these ophiolites go undetected.

In this paper we document the internal structure of the eclogite-facies Monviso ophiolite (MO hereafter) in the Western Alps (Fig. 1), and show that despite the overprint of high-P subduction zone metamorphism–deformation of its lithological units, this ophiolite displays a well-preserved record of

intra-oceanic extensional tectonics that affected it during the opening of the Ligurian-Piedmont Ocean. We further discuss that the crustal architecture and the occurrence of a talc-and-chlorite schist shear zone (i.e., Baracun Shear Zone of Balestro et al., 2015) in Monviso represent the witness of a Jurassic oceanic core complex development (OCC hereafter), which is documented for the first time in the eclogitized ophiolite units in the Western Alps.

Regional Geology of the Western Alps and the Monviso Ophiolite

The Western Alps (Fig. 1A) evolved between the colliding Adria microplate and the European plate during the late Eocene–early Oligocene. Eastward subduction of the Ligurian–Piedmont oceanic lithosphere during the early Cretaceous – middle Eocene resulted in ophiolite emplacement (Rosenbaum and Lister, 2005 and reference therein), underthrusting of the European continental margin beneath Adria (Platt et al., 1989), and tectonic imbrication along WNW-vergent thrust faults (Ricou and Siddans, 1986). In the central part of the belt, eclogite-facies ophiolite units (e.g. Zermatt-Saas Zone *Auct.*) and blueschist-facies metasedimentary units (Combin Zone and "*Schistes Lustrés*" *Auct.*) are tectonically sandwiched between European and Adriatic continental margin units (Fig. 1A; Dal Piaz et al., 2003).

The MO is exposed in the southern part of the Western Alps (Fig. 1) where it rests tectonically on the Dora Maira Unit that was part of the European continental margin (Dal Piaz et al., 2003), and below the *Queyras Schistes Lustrés*, which consist of carbonaceous metasedimentary rocks with meta-ophiolite bodies (Lombardo et al., 1978; Tricart and Lemoine, 1991). The MO includes Iherzolitic mantle rocks intruded by Middle-Upper Jurassic metagabbros (163±2 Ma; Rubatto and Hermann, 2003). Both the metaperidotites and metagabbros are overlain by tholeiitic metabasaltic lavas and an Upper Jurassic – Lower Cretaceous metasedimentary sequence along major tectonic contacts (Angiboust et al., 2011; Balestro et al., 2013 and reference therein; Fig. 1C). As a result, the MO consists of a pile of superposed tectonic units (Fig. 1C), heterogeneously affected by HP metamorphism (T= 550°C and P=2.6 GPa for the Basal Serpentinite, Lago Superiore and Viso Mozzo lower units; T=480°C and P=2.2 GPa for the Forciolline and Vallanta upper units; Angiboust et al., 2012), formed during three main phases of deformation – metamorphism (Balestro et al., 2015): (a) Paleocene to middle Eocene contractional deformation (D₁), eclogite-facies metamorphism at an E-dipping subduction. S₁ foliation was developed during this phase. (b) late Eocene–early Oligocene continental collision stage, which caused W-vergent thrusting (D₂) and blueschist- to greenschist-facies metamorphic re-equilibration. S₂ foliation and F₂ folds were produced during this phase. (c) middle Oligocene–Miocene crustal exhumation (D₃), uplift and doming of the Dora Maira Unit and westward tilting of the Monviso ophiolite.

We describe below the lower part of the MO, corresponding to the *Basal Serpentinite*, *Lago Superiore* and *Viso Mozzo units*, which display the same peak P-T conditions of metamorphism.

Structure of the Baracun Shear Zone

The Baracun Shear Zone (BSZ) within the MO is best exposed at Colle del Baracun (Figs. 1A–2), where it is marked by up-to tens of meters thick talc- and chlorite-schist rocks, separating metaperidotites and 163±2 Ma metagabbros (Rubatto and Hermann, 2003) in the footwall from metabasalt, and calcschist with ophiolite-derived detrital intercalations in the hanging wall (Figs. 2, 3A–B). Both the hanging wall and footwall assemblages and the BSZ (Figs. 2, 3A–G) are unconformably overlain by a Lower Cretaceous (Lagabrielle, 1994) metasedimentary sequence (i.e. post-extensional succession), which is metamorphosed along with the rest of the assemblage (i.e., HP eclogitic facies metamorphism).

Footwall and hanging wall units of the Baracun Shear Zone

Lithological units in the footwall of the BSZ include massive serpentinite with poorly preserved relics of the original mineral phases and textures. Metagabbroic intrusions are meters to tens of meters thick, and are composed mainly of Mg-Al metagabbro characterized by the occurrence of Cr-omphacite. Less common Fe-Ti metagabbro intrusions occur as meters-thick dikes, and contain eclogitic assemblages of garnet-omphacite-rutile. At the contacts with their host metaperidotites, all metagabbro intrusions are extensively rodingitized. The massive serpentinite immediately beneath the BSZ includes 50-cm- to 1-m-thick mylonitic serpentinite with sheared ophicarbonate veins (Fig. 3H). These carbonate-rich veins, which also crosscut the talc-and-chlorite schist of the BSZ (Figs. 3H-I), are overprinted by S_1 foliation and F_2 folds, constraining the timing of hydrothermal activities to a pre-eclogitic facies metamorphic stage.

The hanging wall units above the BSZ consist mainly of calcschist and metabasaltic rocks. The calcschist defines a wedge-shaped stratigraphic unit, increasing in thickness from several meters to ~70 m away from the BSZ (Figs. 2, 3B). The calcschist mainly consists of carbonates, quartz and white mica, with subordinate textural relics of lawsonite, and hosts lenticular intercalations, up to meters thick, of clast- to matrix-supported metabreccia with clasts of gabbroic material (Fig. 3B), which is laterally gradational into a metasandstone unit (Balestro et al., 2014). To the south (Fig. 2), the hanging wall succession consists mainly of metabasalt that preserves relics of brecciated structures and are characterized by alternating greenish/yellowish levels, comprising albite, epidote and clinozoisite, and dark-green levels of Na-Ca amphibole, garnet and chlorite. They are in tectonic contact with calcschists along a late-Alpine, NW-SE striking transtensional fault, which juxtaposes the overturned and upright limbs of a D2 macro-scale fold.

Shear zone rocks and their mineralogy

Decimeter- to several meter-wide blocks of Mg-Al and Fe-Ti metagabbros are embedded in a talc- and chlorite-schist matrix within the BSZ (Figs. 3A-B). These blocks are lithologically similar to the metagabbro intrusions in the footwall metaperidotites. Importantly, there is no material within the BSZ that was derived from the post-extensional Lower Cretaceous metasedimentary succession or metabasaltic rocks. Metagabbro blocks are draped by a clast-supported, several-dm-thick mafic metabreccia (Figs. 3O-P). Clasts and the matrix in this metabreccia are also made of metagabbros as in the blocks, and the entire metabreccia horizon and the gabbroic blocks are foliated (S_1) and folded (F_2) (Fig. 3P; Balestro et al., 2015). These structural relationships clearly constrain the brecciation process as having occurred before the D1 deformation stage (i.e., before eclogitic facies metamorphic stage).

Rocks within the BSZ show different chlorite-, talc-, and amphibole-rich domains (Figs. 3L-M), which are deformed by F_2 folds (see Figs. 3M-N). Chlorite-rich domains consist of chlorite, magnetite, pistacite and accessory apatite, magnetite, allanite, and zircon. Talc-rich domains are composed of talc and fine-grained magnetite, whereas amphibole-rich domains include fine-grained, light-green amphibole and minor chlorite. Calcite locally occurs between these different domains. Our EMP (electron micro-probe) mineral chemistry analyses have shown that (i) talc is characterized by a negligible substitution of Mg by Fe ($X_{Fe}=[0,04-0,09]$), (ii) chlorite has a penninite (i.e., Mg-rich solid solution between serpentine and amesite) composition ($X_{Mg}=[0,88-0,95]$), (iii) amphibole generally belongs to the tremolite-actinolite series, and (iv) talc and chlorite are characterized by high Cr and Ni concentrations. The highest concentrations of Cr and Ni ($Cr_2O_3=0.23$ wt.% and $NiO=0.32$ wt.% in talc; $Cr_2O_3=1.75$ wt.% and $NiO=0.33$ wt.% in chlorite) occur in the core of zoned, coarse-grained talc and chlorite grains and, particularly, within pre-D1 talc and chlorite lamellae included in apatite grains. Talc and chlorite also have a relatively high chlorine content (up to 900 ppm and 500 ppm, respectively).

Unconformable sealing of the Baracun Shear Zone

The BSZ and related hanging wall and footwall units are unconformably overlain by alternating, cm- to dm-thick layers of calcschist, marble and quartz-schist, devoid of any ophiolite-derived detrital material (Figs. 3A-G). The age of these metasedimentary rocks, which thus represent a post-extensional succession (i.e., post-rift), was constrained as the early Cretaceous by Lagabriele (1994) based on a correlation with other sections of the Western Alps, and comparison with the unmetamorphosed stratigraphic succession in the Northern Apennines (e.g. Decandia and Elter, 1972). The basal contact between this succession and both the underlying calcschist alternating with ophiolite-derived horizons of the hanging wall (i.e., Curbarant and East of Colle del Baracun), and the talc- and-chlorite schist of the BSZ (Colle del Baracun and South of Curbarant) is sharp (Figs. 3C-E, 3G), and corresponds to a depositional surface as inferred from the lack of any mylonitic structure associated with it (Fig. 3F). Furthermore, field observations clearly show that this unconformable contact is folded together with the BSZ structural architecture (including hanging wall and footwall units) due to the superposition of D1 and D2 stages (Fig. 2). Collectively, these structural data constrain the slip and faulting activities along the BSZ to the pre – early Cretaceous.

Monviso Ophiolite and the BSZ as a Jurassic Oceanic Core Complex

We interpret the MO and the BSZ as an oceanic core complex (OCC), and discuss below several independent lines of evidence for its origin (Fig. 4). In our model, the lherzolitic peridotites in the footwall of the BSZ represent an exhumed lithospheric mantle. They were intruded by gabbroic dikes – plutons, whose magmas were produced by decompressional melting of the asthenosphere during its slow upwelling. Basaltic lavas and the Upper Jurassic clastic rocks in the hanging wall represent a syn-extensional (i.e., *syn-rift*) sequence resting on the peridotites and gabbros. These processes are reminiscent of those that produce OCCs, in which deformed older rocks are tectonically overlain along detachment faults by relatively undeformed, younger syn-tectonic sediments and basaltic lava flows (e.g. Miranda and Dilek, 2010; Manatschal et al., 2011 for ancient orogenic belts; e.g., Cann et al., 1997; Tucholke et al., 1998; Cannat et al., 2006; Smith et al., 2014 for present-day oceanic settings).

Baracun Shear Zone – a low-angle extensional detachment fault

The architecture of the BSZ, the nature of the contacts with hanging wall and footwall rocks, and the types of fault rocks suggest a simple-shear mode for the kinematics of extension along this originally low-angle shear zone. We interpret the BSZ (up-to tens of meters thick and several hundreds of meters long in outcrop) as the northern segment of a major shear zone, which is tens of kilometers in length and tens to hundreds of meters in thickness (i.e., the *Lago Superiore Shear Zone* of Balestro et al., 2013, and *Lower Shear Zone* of Angiboust et al., 2011). This major shear zone is reminiscent of, both in length and thickness, detachment faults associated with modern OCCs that range from few kilometers up to tens of kilometers in length and up to one hundred of meters in thickness (e.g., Karson et al., 2006; Smith et al., 2014). Our major shear zone, which was intensely folded and thickened during subduction and collisional stages (Fig. 4C), characterizes the lower tectonic units of the MO that were affected by the same peak metamorphic PT conditions (Angiboust et al., 2012). It occurs in the same structural position along its N-S strike, and separates mafic-ultramafic rock units (i.e., serpentinite, metagabbros and meta-ophi-carbonate of the *Basal Serpentinite Unit*) in the footwall from different assemblages of metabasalts, metagabbros and metasedimentary rocks (i.e., the *Viso Mozzo Unit*) in its hanging wall (Fig. 4C).

Metamorphic mineralogy of the BSZ rocks as a result of hydrothermal metasomatism

We posit that the talc- and-chlorite schist within the BSZ originally formed metasomatically as a result of rock–fluid interactions between gabbros, serpentinite and seawater-derived hydrothermal fluids along an OCC-related detachment fault. We remark that the Lower Cretaceous post-extensional sequence sealing the BSZ and the hanging wall and footwall units do not display any structural and textural evidence of metasomatic processes and mineral assemblages, as it would be expected if faulting occurred during subduction and/or the collisional Alpine-related stages.

The texture and composition of the talc- and-chlorite schist within the BSZ are quite similar to those observed in hydrothermally metasomatized oceanic rocks along the detachment fault zone in the Atlantis Massif core complex at the Mid-Atlantic Ridge (Mével, 2003; Boschi et al., 2006; Miranda and Dilek, 2010). Amphibole and chlorite in these rocks were produced from a gabbroic source, whereas talc from serpentinite. The existence of Cl-bearing minerals in the BSZ rocks indicates the occurrence of seawater-derived hydrothermal fluids percolating along–across the shear zone. As documented from the Atlantis Massif and other OCCs (Boschi et al., 2006), silica-enriched hydrothermal fluids, which were produced from gabbro-seawater interactions, reacted with serpentinites leading to talc formation.

Although talc and chlorite recrystallized during Alpine metamorphism, we can still distinguish them due to their high Ni and Cr concentrations in the cores of zoned, coarse-grained crystals and, particularly, within talc and chlorite lamellae included in apatite grains. Apatite, along with other accessory minerals such as magnetite and zircon, represents a pre-Alpine mineral phase, reworked from peridotites and gabbros. Its occurrence constrains the timing of crystallization of talc and chlorite inclusions to a pre-D1 stage. These high Ni and Cr concentrations are compositionally similar to those of chlorite and talc, documented from detachment zone fault rocks in both modern (Boschi et al., 2006) and ancient (Manatschal et al., 2011) OCCs.

The occurrence of pre-S1 carbonate-rich fillings, both at the base of the BSZ (i.e., footwall – BSZ interface; Fig. 3I) and within the talc- and-chlorite schist rocks, also constraints the timing of the responsible metasomatic processes to an intra-oceanic faulting episode. These carbonate-rich fillings, which are homogeneously distributed both along-strike and down-dip of the shear zone, represent the artifacts of seafloor hydrothermal activities as evidenced by our $\delta^{13}\text{C}$ Carbon and $\delta^{18}\text{O}$ Oxygen stable isotope data. The stable isotope values range from -2.80 to <+1.89 for $\delta^{13}\text{C}_{\text{VPDB}}$ and from +11.80 to <+17.79 for $\delta^{18}\text{O}_{\text{VSMOW}}$. The $\delta^{13}\text{C}_{\text{VPDB}}$ values are similar to those of marine carbonates, and the $\delta^{18}\text{O}_{\text{VSMOW}}$ values are closely comparable to those documented from ophiolites associated with the ophiolites in the Alps, Apennines, and Pyrenees (Clerc et al., 2013). The obtained $\delta^{13}\text{C}_{\text{VPDB}}$ and $\delta^{18}\text{O}_{\text{VSMOW}}$ values are different from those of syn-tectonic fluids along subduction zones (e.g. Yamaguchi et al., 2012), and also show that the BSZ fault rocks were not involved in pervasive decarbonation processes and related open-system devolatilization.

Syn-extensional sedimentary sequence in the BSZ hanging wall

Formation of the metabreccia horizons, which drape metagabbro blocks within the BSZ, was spatially and temporally associated with extensional deformation along the shear zone. Gabbroic intrusions experienced cataclastic deformation along the tectonically active extensional BSZ. The process of formation of metabreccia horizons is comparable with those described for gabbro bodies deformed along detachment faults in the Mid-Atlantic Ridge (e.g., Boschi et al., 2006). Their brecciated products progressively exposed in a bathymetric high on the footwall of this shear zone, providing detrital material to an accommodation space in the hanging wall (Fig. 4A, 4B). Multiple occurrences of detrital intercalations in different stratigraphic positions within the syn-extensional sedimentary sequence in the hanging wall block may correspond to discrete episodes of faulting and slip along the BSZ. Similar extensional breccias have been described from the Atlantis Massif core

complex along the Mid-Atlantic Ridge (Karson et al., 2006). The primary, depositional and extensional deformation textures of the metabreccia unit were overprinted by the S_1 foliation (Fig. 3P), which developed during the eclogite-facies metamorphism and related deformation in a subduction zone.

Post-extensional sedimentary sequence

The Lower Cretaceous sedimentary assemblage (i.e., alternating layers of calcschist, marble, and quartz-schist) unconformably covering the footwall–hanging wall rock units and the BSZ represents a post-extensional succession (i.e., *post-rift*) that was folded during the Alpine deformation phase, together with the BSZ and its hanging wall and footwall units. Its depositional age constrains the timing of the faulting and associated shearing as the pre-early Cretaceous (Fig. 4A). Its protolith was deposited on exhumed upper mantle peridotites. Coeval *post-extensional* lithologies also occur in the Western Alps (e.g., Lagabriele, 1994) and in the non-metamorphosed successions in the Central Alps and the Northern Apennines (e.g., Decandia and Elter, 1972). The Valanginian–early Aptian siliciclastic rocks interfingering with carbonate-rich turbiditic deposits in the Deep Galicia Margin (Winterer et al., 1988) represent an excellent *in-situ* analogue for the *post-rift* succession we describe from the Western Alps. These *post-rift* sequences in the Deep Galicia Margin mark the critical timing of the separation of Iberia from the Grand Banks of Canada and the formation of the oldest oceanic crust in the North Atlantic Ocean (Winterer et al., 1988).

Conclusions

This study documents, for the first time, the occurrence in the eclogitized units of the Western Alps of an ancient OCC, comparable with those described from the modern Mid-Atlantic Ridge. Represented by the MO, this ancient OCC reflects the rift-drift history of the Ligurian-Piedmont Ocean basin, which never reached a mature stage (see Lombardo et al., 2002).

The internal structure of the MO and the BSZ display a primary, rift-drift related extensional tectonic architecture (Dilek and Furnes, 2014). However, the complex juxtaposition of the lithological units along–across the BSZ, the incomplete pseudostratigraphy of the MO, and the existence of mafic metabreccia outcrops have led some researchers to suggest that this ophiolite represents either a fossilized subduction channel with a serpentinite-matrix (Guillot et al., 2009), or a fragment of the Jurassic Piedmont oceanic lithosphere crosscut by discrete eclogite-facies shear zones (Angiboust et al., 2011). These existing models interpret the structure of the MO primarily as a result of subduction zone tectonics that was acquired after the development of oceanic lithosphere at a mid-ocean ridge setting within a mature Ligurian – Piedmont Ocean. Our study has shown, however, that the MO displays a well preserved record of extensional detachment faulting that exhumed the lithospheric mantle and produced an OCC during the initial stages of the development of the Jurassic Ligurian-Piedmont Ocean. This OCC subsequently experienced a strong overprint of subduction zone and continental collision tectonics. The multiply deformed MO in the Western Alps indicates that incomplete and highly deformed meta-ophiolitic successions that are juxtaposed across major shear zones in high-P belts do not always represent the product of a subduction channel, even though that is where and how they might have come up after going down during ocean closure.

Acknowledgments

We thank Science Editors Arlo B. Weil and Eric Kirby for their careful editorial handling. We would like to express our sincere thanks to reviewers J. Wakabayashi and M. Marroni, and an anonymous referee for their constructive and thorough reviews, from which we have benefited greatly in revising

our manuscript. We also thank S. Cavagna, who accurately processed samples for isotopic analyses. This research has been supported by “ex 60%–2013 and 2014” (Università degli Studi di Torino, grants to A. Festa) and the Italian Ministry of University and Research (Cofin-PRIN 2010/2011 “GEOPROB – GEodynamic Processes of Oceanic Basins”, grant no. [2010AZR98L_002] – G.A. Pini, to A. Festa, and grant no. [2010AZR98L_008] – M.I. Spalla, to P. Tartarotti; Cofin-PRIN 2010/2011 “Subduction and exhumation of continental lithosphere: implications on orogenic architecture, environment and climate” grant - R. Carosi, to G. Balestro).

361

362 **References**

- 363 Angiboust, S., Agard, P., Raimbourngh, H., Yamato, P., and Huet, B., 2011, Subduction interface
364 processes recorded by eclogite- facies shear zones (Monviso, W. Alps): *Lithos*, v.127, p.222–
365 238.
- 366 Angiboust, S., Langdon, R., Agard, P., Waters, D., and Chopin, C., 2012, Eclogitization of the
367 Monviso ophiolite and implications on subduction dynamics: *Journal of Metamorphic*
368 *Geology*, v.30, p.37–61.
- 369 Balestro, G., Festa, A., and Tartarotti, P., 2015, Tectonic significance of different block-in-matrix
370 structures in exhumed convergent plate margins: examples from oceanic and continental HP
371 rocks in Inner Western Alps (northwest Italy): *International Geology Review*, v.57(5-8),
372 p.581-605.
- 373 Balestro, G., Fioraso, G. and Lombardo, B., 2013, Geological map of the Monviso massif (Western
374 Alps): *Journal of Maps*, v.9, p.623-634.
- 375 Balestro, G., Lombardo, B., Vaggelli, G., Borghi, A., Festa, A., and Gattiglio, M., 2014,
376 Tectonostratigraphy of the Northern Monviso Meta-ophiolite Complex (Western Alps): *Italian*
377 *Journal of Geosciences*, v.133 (3), p.409-426.
- 378 Boschi, C., Früh-Green, G.L., and Delacour, A., 2006, Mass transfer and fluid flow during detachment
379 faulting and development of an oceanic core complex, Atlantis Massif (MAR 30°N):
380 *Geochemistry, Geophysics, Geosystems*, v.7, doi: 10.1029/2005GC001074.
- 381 Cann, J.R., Blackman, D.K., Smith, D.K., McAllister, E., Janssen, B., Mello, S., Avgerinos, E., Pascoe,
382 A.R., and Escartín, J., 1997, Corrugated slip surfaces formed at ridge-transform intersections
383 on the Mid-Atlantic Ridge: *Nature*, v.385, 329–332.
- 384 Cannat, M., 1993, Emplacement of mantle rocks in the sea floor at mid-ocean ridges: *Journal of*
385 *Geophysical Research*, v.98, 4163–4172.
- 386 Cannat, M., Sauter, D., Mendel, V., Ruellan, E., Okino, k., Escartin, J., Combier, v., and Baala, M.,
387 2006, Modes of seafloor generation at a melt-poor ultraslow-spreading ridge: *Geology*, v.34(7),
388 605–608.
- 389 Clerc, C., Boulvais, P., Lagabrielle, Y., and De Saint Blanquat, M., 2013, Ophicalcites from the
390 northern Pyrenean belt: a field, petrographic and stable isotope study: *International Journal of*
391 *Earth Sciences*, v.103 (1), p.141-163.
- 392 Dal Piaz, G.V., Bistacchi, A., and Massironi, M., 2003, Geological outline of the Alps: *Episodes*, v.26,
393 p.175–180.

- 394 Decandia, F.A., and Elter, P., 1972, La “zona” ofiolitifera del Bracco nel settore compreso fra Levante
395 e la Val Graveglia (Appennino Ligure): Memorie della Societa Geologica Italiana, v.XI,
396 p.503–530.
- 397 Dilek Y., and Furnes, H., 2014, Ophiolites and their origins: Elements, v.10, p. 93-100.
- 398 Dilek, Y., and Thy, P., 1998, Structure, petrology and seafloor spreading tectonics of the Kizildag
399 ophiolite, Turkey. In: Mills, R.A., Harrison, K. (Eds.), Modern Ocean Floor Processes and the
400 Geological Record, 148. Geological Society, London, pp. 43–69. Special Publication.
- 401 Dilek, Y., Ophiolite concept and its evolution: In, Geological Society of America Special Paper 373, p.
402 1-16.
- 403 Guillot, S., Hattori, K., Agard, P., Schwartz, S., and Vidal, O., 2009, Exhumation processes in oceanic
404 and continental subduction contexts: A review, *in* Lallemand, S., and Funiciello, F., eds.,
405 Subduction zone geodynamics: Springer-Verlag Berlin Heidelberg, p.175-205.
- 406 Karson, J.A., Früh-Green, G.L., Kelley, D.S., Williams, E.A., Yoerger, D.R., and Jakuba, M., 2006,
407 Detachment shear zone of the Atlantis Massif core complex, Mid-Atlantic Ridge, 30°N:
408 Geochemistry, Geophysics, Geosystems, v.7, Q06016, doi:10.1029/2005GC001109.
- 409 Lagabriele, Y., 1994, Ophiolites of the southwestern Alps and the structure of the Tethyan oceanic
410 lithosphere: *Ofioliti*, v. 19, p. 413–434.
- 411 Lombardo, B., Nervo, R., Compagnoni, R., Messiga, B., Kienast, J., Mevel, C., Fiora, L., Piccardo, G.,
412 and Lanza, R., 1978, Osservazioni preliminari sulle ofioliti metamorfiche del Monviso (Alpi
413 Occidentali): *Rendiconti della Società Italiana di Mineralogia e Petrologia*, v. 34, p. 253–305.
- 414 Lombardo, B., Rubatto, D., and Castelli, D., 2002, Ion microprobe U–Pb dating of zircon from a
415 Monviso metaplagiogranite: Implications for the evolution of the Piedmont-Liguria Tethys in
416 the Western Alps: *Ofioliti*, v.27, p.109–117.
- 417 Manatschal, G., Sauter, D., Karpoff, A.M., Masini, E., Mohn, G., and Lagabriele, Y., 2011, The
418 Chenalliet Ophiolite in the French/Italian Alps: An ancient analogue for an oceanic core
419 complex?: *Lithos*, v.124, p.169-184.
- 420 Mével, C., 2003, Serpentinization of abyssal peridotite at mid-ocean ridges: *Comptes Rendus*
421 *Geosciences*, v. 335, p. 825–852.
- 422 Miranda, E.A., Dilek, Y., 2010, Oceanic Core Complex Development in Modern and Ancient Oceanic
423 Lithosphere: Gabbro-Localized versus Peridotite-Localized Detachment Models: *Journal of*
424 *Geology*, v.118, p. 95-109.
- 425 Platt, J.P., Behrmann, J.H., Cunningham, P.C., Dewey, J.F., Helman, M., Parish, M., Shepley, M.G.,
426 Wallis, S., and Western, P.J., 1989, Kinematics of the Alpine arc and the motion history of
427 Adria: *Nature*, v. 337, p. 158–161.
- 428 Rosenbaum, G., and Lister, G.S., 2005, The Western Alps from the Jurassic to Oligocene: spatio-
429 temporal constraints and evolutionary reconstructions: *Earth-Science Reviews*, v. 69, p. 281–
430 306.

- 431 Ricou, L.E., and Siddans, W.B., 1986, Collision tectonics in the western Alps: Geological Society,
432 London, Special Publications, v.19, p. 229–244.
- 433 Rubatto, D. and Hermann, J., 2003, Zircon formation during fluid circulation in eclogites (Monviso,
434 Western Alps): Implications for Zr and Hf budget in subduction zones: *Geochimica et*
435 *Cosmochimica Acta*, v. 67, p. 2173–2187.
- 436 Smith, D.K., Schouten, H., Dick, H.J.B., Cann, J.R., Salters, V., Marschall, H.R., Ji, F., Yoerger, D.,
437 Sanfilippo, A., Parnell-Turner, R., Palmiotto, C., Zheleznov, A., Bai, H., Junkin, W., Urann,
438 B., Dick, S., Sulanowska, M., Lemmond, P., and Curry, S., 2014, Development and evolution
439 of detachment faulting along 50 km of the Mid-Atlantic Ridge near 16.5°N: *Geochemistry*
440 *Geophysics Geosystems*, v.15, p.4692–4711.
- 441 Tricart, P., and Lemoine, M., 1991, The Queyras ophiolite west of Monte Viso (Western Alps):
442 indicator of a peculiar ocean floor in the Mesozoic Tethys: *Journal of Geodynamics*, v.13,
443 p.163–181.
- 444 Tucholke, B.E., Lin, J., and Kleinrock, M.C., 1998, Megamullions and mullion structure defining
445 oceanic metamorphic core complexes on the Mid-Atlantic Ridge: *Journal of Geophysical*
446 *Research*, v. 103 (B5), p. 9857–9866.
- 447 Winterer, E.L., Gee, J.S., and Van Waasbergen, R.J., 1988, The source area for Lower Cretaceous
448 clastic sediments of the Galicia Margin: geology and tectonic and erosional history, *in* Boillot,
449 G., Winterer, E.L., et al., *Proc. ODP, Scientific Results*, v.103: College Station, TX (Ocean
450 Drilling Program), p. 697–732.
- 451 Yamaguchi, A., Ujiie, K., Nakai, S., and Kimura, G., 2012, Sources and physicochemical
452 characteristics of fluids along a subduction-zone megathrust: A geochemical approach using
453 syn-tectonic mineral veins in the Mugli mélange, Shimanto accretionary complex.
454 *Geochemistry, Geophysics, Geosystems*, v. 13(1).

455

456 **Figure captions**

457

458 **Figure 1** – (A) Simplified tectonic map of the Western Alps. (B) Location of Figure 1A. (C)
459 Representative structural cross section of the Monviso (modified from [Angiboust et al., 2011](#); [Balestro](#)
460 [et al., 2013](#)).

461

462 **Figure 2** – (A) Geological map of the Colle del Baracun section, (B) cross-section depicting the
463 geometry of the BSZ.

464

465 **Figure 3** – (A) Panoramic view, and (B) line drawing of the Baracun Shear Zone (BSZ). Post-
466 extensional sedimentary sequence resting unconformably on the talc- and chlorite-schist of the BSZ,
467 serpentinite and syn-extensional sequence. (C, D, E) Views of the post-extensional sequence
468 unconformably resting on the BSZ. Note that in Fig. 3E, the sequence is overturned. (F)
469 Photomicrograph of a marble layer occurring in the Lower Cretaceous metasedimentary succession,
470 few cm above the contact with the talc- and-chlorite schist of the BSZ. The marble is poorly foliated
471 and calcite crystals show a weakly deformed granoblastic texture. Key to lettering: Wmca: white mica,

472 Cal: calcite, Qtz: quartz. (G) Post-extensional metasedimentary rocks unconformably overlying the
 473 syn-extensional metasedimentary units. (H) Close-up view of the overturned tectonic contact between
 474 the massive serpentinite in the footwall and the BSZ. Note the progressive transition from massive
 475 serpentinite to pervasively sheared talc- and chlorite- schist. (I) Close-up of the sheared ophicalcite of
 476 Fig. 3H, showing a carbonate vein overprinted by S1 foliation (dashed white line) and deformed by D2
 477 folds (dashed black line). (L) Structural fabric in the talc- and chlorite-schist matrix of the BSZ. (M)
 478 Rootless D2 fold hinges in chlorite-rich (Chl) domains of the talc- and chlorite-schist overprinting the
 479 early S1 foliation (dashed white lines). S2 axial plane foliation (dashed black lines) occurring in talc-
 480 rich (Tlc) domains (hand sample). (N) Photomicrograph of talc- and-chlorite schist in the BSZ,
 481 showing amphibole- (Amp), chlorite- (Chl) and talc-rich (Tlc) domains folded by tight to isoclinal D2
 482 folds; note the folded S1 foliation (dashed white lines). (O) Close-up of a Fe-Ti metagabbro block
 483 within the BSZ; arrows point to a clast-supported mafic metabreccia comprising gabbroic clasts of the
 484 same composition. (P) Close-up view of the mafic metabreccia of Fig. 3O. Note that cm-sized,
 485 irregularly shaped clasts preserve an earlier foliation (S1) deformed by D2 folds. (Q) A Mg-Al
 486 metagabbro block in the BSZ, enveloped by the talc- and-chlorite schist matrix (arrows). (R) The talc-
 487 and-chlorite matrix includes gabbroic clasts wrenched by faulting along the BSZ.

488
 489 **Figure 4** – (A) Interpretive cross section for the development of the oceanic core complex, BSZ and
 490 syn- and post-extensional sequences in the MO. (B) Close-up of the BSZ, depicting the inferred
 491 tectonic and hydrothermal processes. (C) Close-up of the representative cross-section of Fig. 1C,
 492 depicting at a regional scale the prolongation of the BSZ within the MO lower tectonic units.

494

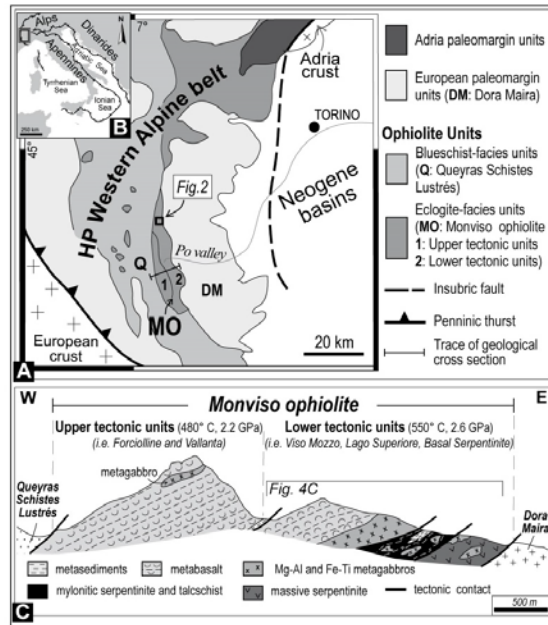


Figure 1 - Festa et al.

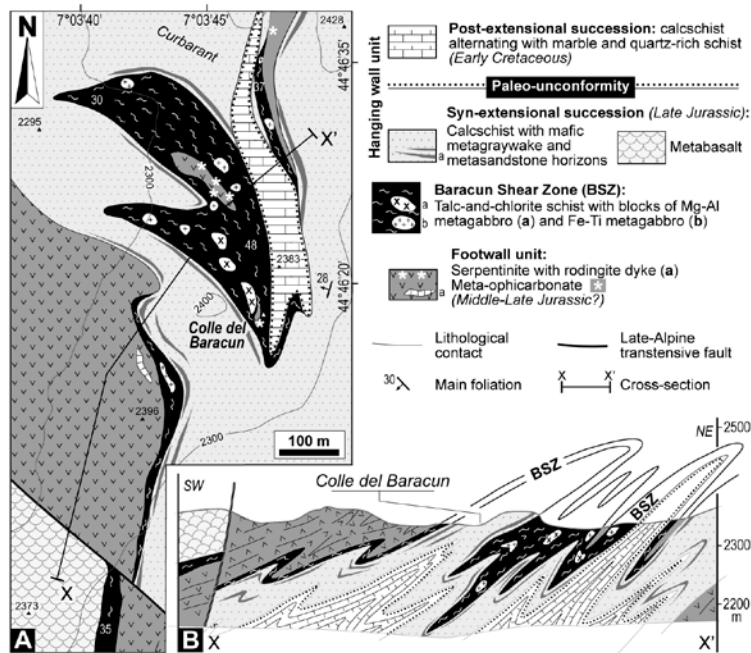


Figure 2 - Festa *et al.*

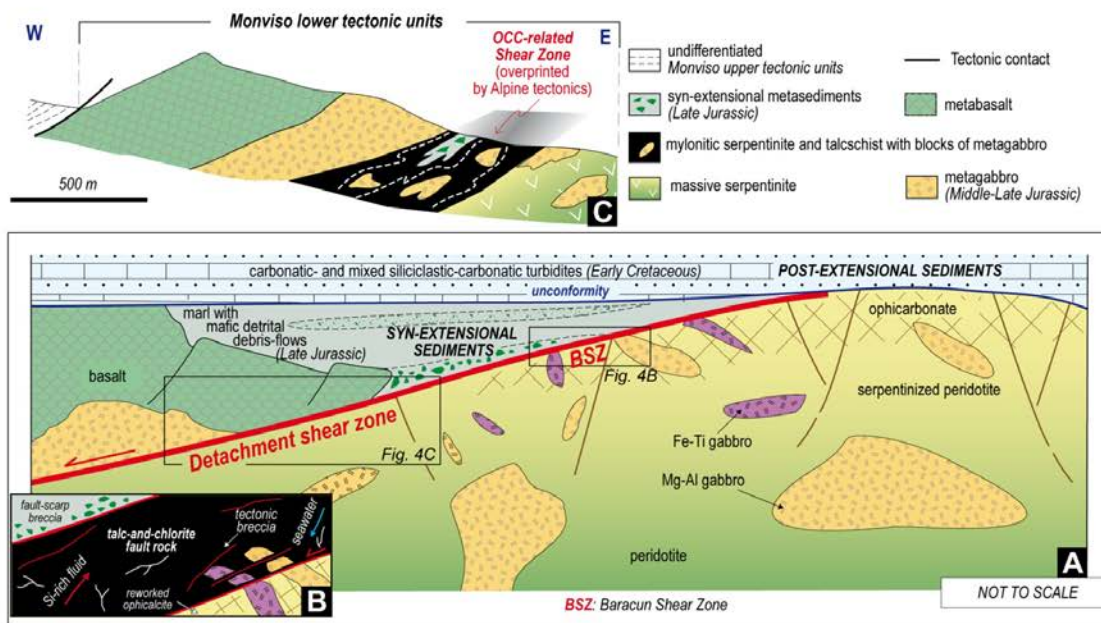


Figure 4 - Festa et al.